



Multimodal Contextualized Support for Enhancing Video Retrieval System

Quoc-Bao Nguyen-Le^{1,2}  and Thanh-Huy Le-Nguyen² 

¹ Research Lab of Center of Talents in AI

² Software Engineering Lab, VNU-HCM

Abstract. Current video retrieval systems, especially those used in competitions, primarily focus on querying individual keyframes or images rather than encoding an entire clip or video segment. However, queries often describe an action or event over a series of frames, not a specific image. This results in insufficient information when analyzing a single frame, leading to less accurate query results. Moreover, extracting embeddings solely from images (keyframes) does not provide enough information for models to encode higher-level, more abstract insights inferred from the video. These models tend to only describe the objects present in the frame, lacking a deeper understanding. In this work, we propose a system that integrates the latest methodologies, introducing a novel pipeline that extracts multimodal data, and incorporate information from multiple frames within a video, enabling the model to abstract higher-level information that captures latent meanings, focusing on what can be inferred from the video clip, rather than just focusing on object detection in one single image.

1 Introduction

We leverage state-of-the-art (SOTA) vision-language models such as Nomic [8], Uform, and OpenClip [10] to extract keyframe embeddings and align them with text. Since most video retrieval queries are text-based, we transform the problem from querying with images to querying with text. To achieve this, we utilize lightweight yet robust language models (LLMs) like Phi3 (English), known for its strong OCR capabilities from Microsoft, and Vintern from 5CD (tailored specifically for Vietnamese). We also employ sentence chunking techniques and incorporate BGM [2] multilingual text embeddings for vector extraction.

However, our key finding is that applying these methods frame by frame does not perform well when handling queries that describe a sequence of frames (a clip). These methods tend only to describe the objects within a single frame, failing to infer the meaningful, high-level information in the clip. To address this, we design a pipeline that utilizes audio context to enrich model phi35 with higher-level information over a longer sequence of frames (up to 20), making it more suitable for most queries. Other video-encoding methods (e.g., ViClip and VideoIntern [14]) are also incorporated into our system.

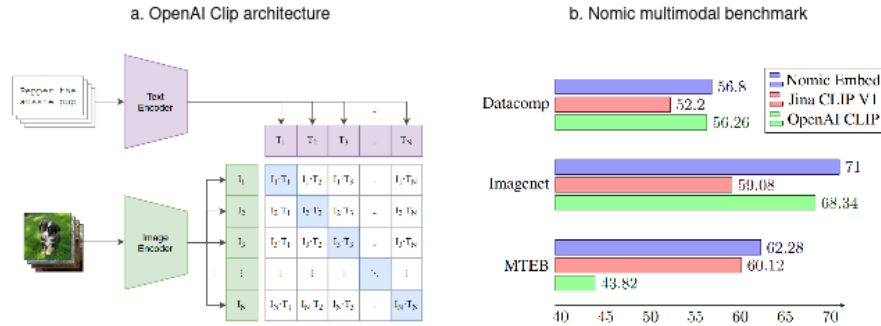


Fig. 1. The architecture of the CLIP model is shown on the left. However, Nomic Vision outperforms CLIP across all benchmarks. Our experience also confirms that Nomic is significantly superior to CLIP in visual-language retrieval tasks.

Throughout the paper, we analyze the improved results achieved by our approach. In Section 3, we present and scientifically analyze the methodologies used in our system. Section 4 focuses on the technical architecture, including the backend and frontend of the system. Finally, Section 5 offers a summary, discussion, and suggestions for future work.

2 Related Work

3 Our approach

3.1 Image Deduplication with Dinov2

Even after extracting keyframes from a video, many frames can still be nearly identical. For instance, with news video, frames featuring reporters with the same background, attire, and posture often repeat between transitions in news videos. Similarly, introductory frames tend to reappear later, adding little value to the query process. This occurs because keyframe extraction algorithms typically compare consecutive frames locally, without considering long-term global similarities, leading to unnecessary duplication in the dataset. While classical deduplication methods like hashing (e.g., PHash, DHash [13]) exist, deep learning-based approaches enable more effective comparisons. Using average pooling with CNN models like ResNet [6] helps identify duplicates, but Dinov2 [9], a transformer-based model trained on unlabeled data using retrieval techniques—proves the most effective for video retrieval tasks due to its ability to compare feature similarity vectors. However, deduplication is applied only within individual videos, not across the entire dataset. Given a dataset of N frames $X_i \in \mathbb{R}^{h \times w \times c}$ and K videos, we process each video V_k by computing the cosine similarity between

frame embeddings extracted by Dinov2:

$$\forall (X_i, X_j) \in V_k : \frac{f(X_i) \cdot f(X_j)}{|f(X_i)| |f(X_j)|} > \delta \rightarrow X_j \in (Re)$$









		A shot of a dog wagging its tail. The dog's head is covered by a wooden grain door. Later, we realize this is a refrigerator. Following that, there is a scene of a person feeding this dog	0.79
		A shot of a playful dog and its owner wrestle in the snowy yard, chasing each other with joyous abandon.	0.05
		A pet dog excitedly runs through the snowy yard, chasing a toy thrown by its owner, then hide in the refrigerator.	0.12
		A playful dog slides down a snowy hill, wagging its tail with delight.	0.04

Fig. 2. Although all the input texts describe a context involving a dog, ViClipB16 accurately interprets the sequence of frames and assigns the highest score to the first text, which also matches the query.

Here, $f(\cdot) \in R^d$ is the feature vector from Dinov2, δ is the deduplication threshold (usually $\delta = 0.9$), and (Re) is the set of frames to remove. We retain only X_i and delete the subsequent duplicate frames X_j within the same video.

3.2 Vision-Language Alignment

We leverage Nomic’s nomic-embed-vision [8], which is trained in a style similar to Locked Image Tuning (LiT), where a high-performing text embedder is frozen, and a vision encoder is fine-tuned from a pretrained checkpoint. In benchmark comparisons, Nomic Embed v1.5 is the only multimodal encoder to outperform OpenAI CLIP ViT B/16 and Jina CLIP v1 on both text and multimodal benchmarks. It leads in Imagenet Zero-Shot, Datacomp’s 38 zero-shot multimodal evaluations, and MTEB for text embedding performance. In addition, we utilize Uform, a lightweight multimodal AI model capable of content understanding and generation across multilingual texts, images, and soon, video. Uform operates up to 5x faster than OpenAI’s CLIP and LLaVA, making it ideal for scalable applications. We also include the baseline provided by most retrieval competitions, Clip-Base32 [3], but we still find that the two methods mentioned earlier still produce better results.

3.3 Text Description from LLMs

Since most queries are in text format, we shift our focus from image queries to text queries. Each image is paired with a descriptive text, allowing us to compare it against the query through feature extraction. We choose to employ

Vintern [4] because of its capability to provide detailed image descriptions based on knowledge of Vietnam. This model utilizes a patch-based approach, breaking the input image into smaller segments and focusing on each patch to ensure no important details are overlooked.

We also select Phi-3-vision [1] for its lightweight, state-of-the-art architecture, trained on datasets that include synthetic data and filtered publicly available content. This model emphasizes high-quality, reasoning-rich data for both text and vision tasks. Additionally, we utilize BGM due to its multilingual capabilities, eliminating language differences concerns. It supports semantic retrieval across more than 100 languages and can process inputs of varying granularity, from short sentences to long documents of up to 8,192 tokens.

Prompted Object Detection We have prepared a sparse vector database for object detection using YOLOv8 [12], pretrained on OpenImageV7, with 600 object classes denoted as:

$$V = \{v_i \in \{0, 1\} | 0 \leq i < C\}$$

For a text query such as, *"A man is answering questions in an interview at a festival. Behind him is a decorative item shaped like a purple bird"* the model detects the classes "man" and "bird," returning a vector $q = [0, 1, \dots, 0, 1, \dots]$. This vector is then compared against the sparse vector database V to filter out irrelevant results.

3.4 Video-Level Representation

Since representation from a series of frames is important, we choose to use ViClipB16, ViClipL14, and VideoIntern [14]. They are part of the InternVideo framework, a versatile video foundation model that excels by integrating generative and discriminative learning techniques, resulting in state-of-the-art performance across various video understanding tasks.

The framework utilizes both masked video modeling (generative) and contrastive video-language learning (discriminative), effectively merging these approaches to enhance video representation learning. InternVideo employs a masked video encoder with modules for local temporal and global spatiotemporal interactions. This architecture efficiently scales by reusing pre-trained Vision Transformers (ViTs) from image-text data, streamlining multimodal learning and enhancing performance.

Figure 3 displays an example of these models' ability to differentiate concepts of continuous activities. However, these models can only encode information from 8 consecutive frames.

3.5 High-Level Abstraction

While the model can detect and identify objects within frames, it struggles to infer higher-level abstractions, such as activities, actions, or emotions across individual frames and sequences. To address this limitation, we provide additional

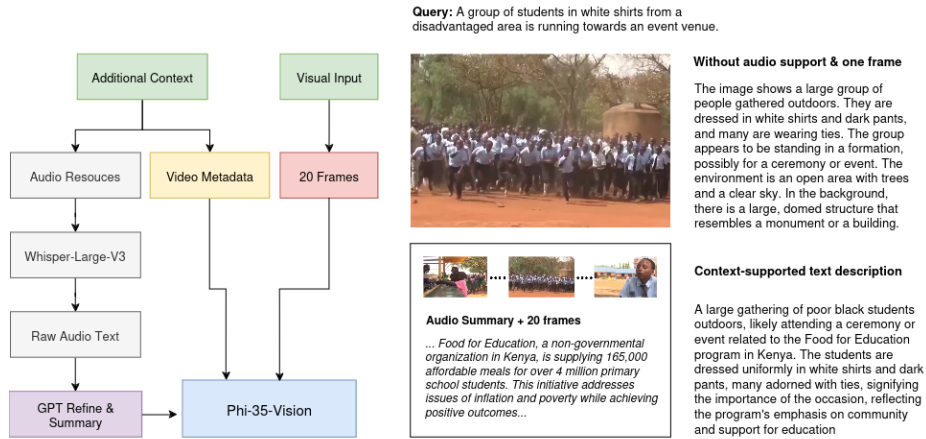


Fig. 3. Phi-35, enhanced with contextualized audio summaries, can grasp the high-level concepts behind a clip, making it well-suited for complex and abstract queries.

context to the model by incorporating processed audio. This audio is extracted using the Whisper-Large-V3 [11] model, corrected for spelling errors by GPT-4, Gemini, or Llama, and then summarized as segmented clips within a video. For instance, the first five minutes of a video might focus on one topic (one clip), while subsequent segments discuss different subjects. This summarized audio text provides the model with crucial contextual information for inference.

For example, an image with many students in white uniforms running towards the camera. Without the context from neighboring frames and the audio report stating (see figure 3 for details), the model would struggle to grasp a comprehensive, high-level understanding of the situation.

We find this approach notably effective because it is suitable for most queries that describe high-level concepts that viewers can infer while watching a clip. We believe this method is optimal because it captures information from an extended series of frames while enabling the model to understand the overarching meaning of the clip. Currently, the Phi35-vision-instruct model supports multi-image or video clip summarization. The pipeline is detailed in Figure 3.

4 Our System Design

4.1 Vector Database Search

We utilize Faiss [5] [7], developed by Facebook, to optimize the speed of vector searches with built-in methods such as IndexFlatL2 and IndexIVFFlat combined with product quantization. The score is calculated as follows:

$$S = \sum_i^d M(t)[j] \odot IE[:, j]$$

where $M(t) \in \mathbb{R}^d$ represents the query embedding vector, and $M(t)[j]$ denotes the j -th element of the text embedding. Here, $IE \in \mathbb{R}^{N \times d}$ is the image database, and $IE[:, j]$ indicates the j -th element of each image embedding (keyframe). The resulting score $S \in \mathbb{R}^N$ reflects the confidence level of similarity. This method similarly applies when retrieving a clip containing 8 frames (from ViClipB16 or ViClipL14), but the total number of elements N is reduced to $N/8$.

4.2 Score Aggregation

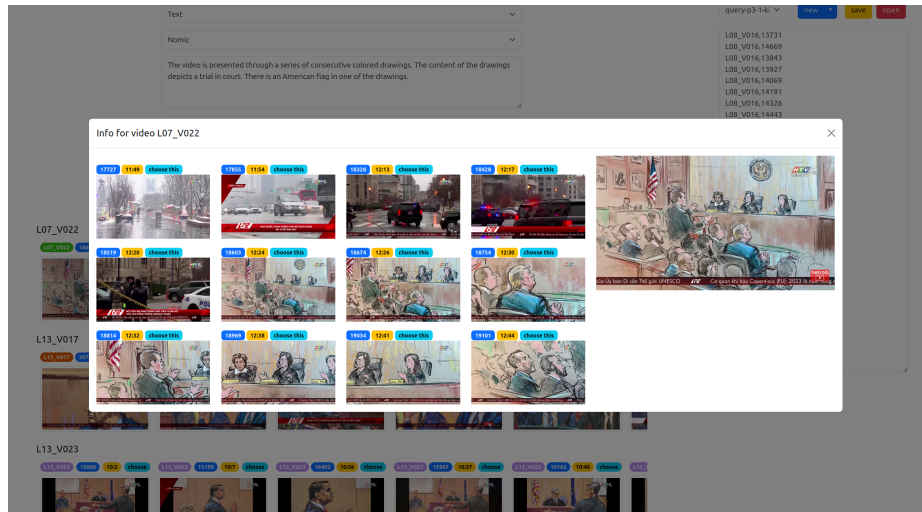


Fig. 4. Query: "The video is presented through a series of consecutive colored drawings. The content of the drawings depicts a trial in court. There is an American flag in one of the drawings". In this example, we select the Nomic method from eight other options to query, and the correct result appears ranked first. When the user clicks on any frame, a modal displays a list of preceding and following frames. On the right side, the video plays at the corresponding timestamp, allowing the user to verify the results. Users can easily click "choose this" and the selected frames are automatically registered to database and displayed on the right submission manager panel.

For models querying images/frames (e.g., Uform, Nomic, OpenClip) and those querying through text descriptions and embeddings (e.g., Phi35, Vintern), the output is $S_i \in \mathbb{R}^N$, representing the confidence for each frame, $\forall i \in I$ for different models. We employ two aggregation methods:

1. Summation of Confidences: We sum the confidence scores, meaning frames predicted accurately by multiple models will have higher scores. We then sort and select the indices of the top T frames:

$$R = \text{argsort}(\sum_{i \in I} S_i)[-T :]$$

2. Unique Frame Selection: In cases where one model predicts a frame correctly while others do not, simply summing scores could exclude valuable frames. Thus, we can use:

$$\text{Set}(\text{argsort}(S_i)[-T :]) \quad \forall i \in I$$

For models returning indices of a series of 8 frames (such as ViClipB16, ViClipL14, VideoIntern), we apply similar aggregation to extract the top T series of frames.

4.3 Result Display

Once we identify the top T potential results, we display the frames on the front-end with clear video categorization: frames from the same video are grouped in a single row and distinguished by a unique color label for easy identification. When users click on a frame, the adjacent 4 frames both before and after will be shown, along with the video playing at the exact moment the keyframe appears. This design allows users to verify results and select the correct answer quickly.

4.4 Supporting Techniques

Occasionally, queries may be less descriptive but mention specific locations (e.g., "Bitexco") or unique symbols (e.g., "Dong Ho paintings"). In such cases, the image search feature leverages URLs from the internet to retrieve the most similar images. This approach is effective if the descriptive text indicates a known image (location, distinctive features, etc.).

However, our error analysis revealed limitations in language models when describing images. For example, when querying an image of a cycle rickshaw, models like Vintern [4], Phi3 [1], and Phi35 merely categorize it as a "three-wheeled vehicle," making it difficult to retrieve frames from queries specifically referencing "cycle rickshaw." To address this, we integrate modules for paraphrasing and translation using the GPT-4O-mini API to simplify expressions into more accessible descriptions suitable for LLMs.

5 Conclusion and Discussion

In this work, we addressed the limitations of existing video retrieval systems that primarily focus on individual frames, which often fail to capture the higher-level insights present in video clips. Introducing a novel pipeline that utilizes multimodal data from sequences of frames enabled more accurate and abstract interpretation of video content. Our system integrates state-of-the-art vision-language models and incorporates audio context to provide models with a broader understanding of actions and events across multiple frames, improving retrieval performance for complex queries.

The system is implemented with a Python Flask API backend and a front-end built using HTML and JavaScript. While this provides a functional interface, there are still limitations in terms of thoroughly browsing and interacting with results. In the future, we aim to enhance the user interface and experience, focusing on making the retrieval process more intuitive and efficient for users. This will allow for a more seamless exploration of the retrieved video segments and further improve the overall system usability.

References

1. Abdin, M., Aneja, J., Awadalla, H., Awadallah, A., Awan, A.A., Bach, N., Bahree, A., Bakhtiari, A., Bao, J., Behl, H., Benhaim, A., Bilenko, M., Bjorck, J., Bubeck, S., Cai, M., Cai, Q., Chaudhary, V., Chen, D., Chen, D., Chen, W., Chen, Y.C., Chen, Y.L., Cheng, H., Chopra, P., Dai, X., Dixon, M., Eldan, R., Fragoso, V., Gao, J., Gao, M., Gao, M., Garg, A., Giorno, A.D., Goswami, A., Gunasekar, S., Haider, E., Hao, J., Hewett, R.J., Hu, W., Huynh, J., Iter, D., Jacobs, S.A., Javaheripi, M., Jin, X., Karampatziakis, N., Kauffmann, P., Khademi, M., Kim, D., Kim, Y.J., Kurilenko, L., Lee, J.R., Lee, Y.T., Li, Y., Li, Y., Liang, C., Liden, L., Lin, X., Lin, Z., Liu, C., Liu, L., Liu, M., Liu, W., Liu, X., Luo, C., Madan, P., Mahmoudzadeh, A., Majercak, D., Mazzola, M., Mendes, C.C.T., Mitra, A., Modi, H., Nguyen, A., Norick, B., Patra, B., Perez-Becker, D., Portet, T., Pryzant, R., Qin, H., Radmilac, M., Ren, L., de Rosa, G., Rosset, C., Roy, S., Ruwase, O., Saarikivi, O., Saied, A., Salim, A., Santacroce, M., Shah, S., Shang, N., Sharma, H., Shen, Y., Shukla, S., Song, X., Tanaka, M., Tupini, A., Vaddamanu, P., Wang, C., Wang, G., Wang, L., Wang, S., Wang, X., Wang, Y., Ward, R., Wen, W., Witte, P., Wu, H., Wu, X., Wyatt, M., Xiao, B., Xu, C., Xu, J., Xu, W., Xue, J., Yadav, S., Yang, F., Yang, J., Yang, Y., Yang, Z., Yu, D., Yuan, L., Zhang, C., Zhang, C., Zhang, J., Zhang, L.L., Zhang, Y., Zhang, Y., Zhang, Y., Zhou, X.: Phi-3 technical report: A highly capable language model locally on your phone (2024), <https://arxiv.org/abs/2404.14219>
2. Chen, J., Xiao, S., Zhang, P., Luo, K., Lian, D., Liu, Z.: Bge m3-embedding: Multi-lingual, multi-functionality, multi-granularity text embeddings through self-knowledge distillation (2024), <https://arxiv.org/abs/2402.03216>
3. Cherti, M., Beaumont, R., Wightman, R., Wortsman, M., Ilharco, G., Gordon, C., Schuhmann, C., Schmidt, L., Jitsev, J.: Reproducible scaling laws for contrastive language-image learning. In: 2023 IEEE/CVF Conference on Computer Vision and Pattern Recognition (CVPR). IEEE (Jun 2023). <https://doi.org/10.1109/cvpr52729.2023.00276>, <http://dx.doi.org/10.1109/CVPR52729.2023.00276>
4. Doan, K.T., Huynh, B.G., Hoang, D.T., Pham, T.D., Pham, N.H., Nguyen, Q.T.M., Vo, B.Q., Hoang, S.N.: Vintern-1b: An efficient multimodal large language model for vietnamese (2024), <https://arxiv.org/abs/2408.12480>
5. Douze, M., Guzhva, A., Deng, C., Johnson, J., Szilvasy, G., Mazaré, P.E., Lomeli, M., Hosseini, L., Jégou, H.: The faiss library (2024)
6. He, K., Zhang, X., Ren, S., Sun, J.: Deep residual learning for image recognition (2015), <https://arxiv.org/abs/1512.03385>
7. Johnson, J., Douze, M., Jégou, H.: Billion-scale similarity search with GPUs. *IEEE Transactions on Big Data* **7**(3), 535–547 (2019)
8. Nussbaum, Z., Duderstadt, B., Mulyar, A.: Nomic embed vision: Expanding the latent space (2024), <https://arxiv.org/abs/2406.18587>

9. Oquab, M., Darcet, T., Moutakanni, T., Vo, H., Szafraniec, M., Khalidov, V., Fernandez, P., Haziza, D., Massa, F., El-Nouby, A., Assran, M., Ballas, N., Galuba, W., Howes, R., Huang, P.Y., Li, S.W., Misra, I., Rabbat, M., Sharma, V., Synnaeve, G., Xu, H., Jegou, H., Mairal, J., Labatut, P., Joulin, A., Bojanowski, P.: Dinov2: Learning robust visual features without supervision (2024), <https://arxiv.org/abs/2304.07193>
10. Radford, A., Kim, J.W., Hallacy, C., Ramesh, A., Goh, G., Agarwal, S., Sastry, G., Askell, A., Mishkin, P., Clark, J., Krueger, G., Sutskever, I.: Learning transferable visual models from natural language supervision (2021), <https://arxiv.org/abs/2103.00020>
11. Radford, A., Kim, J.W., Xu, T., Brockman, G., McLeavey, C., Sutskever, I.: Robust speech recognition via large-scale weak supervision (2022), <https://arxiv.org/abs/2212.04356>
12. Reis, D., Kupec, J., Hong, J., Daoudi, A.: Real-time flying object detection with yolov8 (2024), <https://arxiv.org/abs/2305.09972>
13. Wang, J., Fu, X., Xiao, F., Tian, C.: Dhash: Enabling dynamic and efficient hash tables (2020), <https://arxiv.org/abs/2006.00819>
14. Wang, Y., Li, K., Li, Y., He, Y., Huang, B., Zhao, Z., Zhang, H., Xu, J., Liu, Y., Wang, Z., Xing, S., Chen, G., Pan, J., Yu, J., Wang, Y., Wang, L., Qiao, Y.: Internvideo: General video foundation models via generative and discriminative learning (2022), <https://arxiv.org/abs/2212.03191>